Advanced Powder Technology 28 (2017) 2295–2305

Contents lists available at ScienceDirect

Advanced Powder Technology

journal homepage: www.elsevier.com/locate/apt

Original Research Paper

Free convection of hybrid Al_2O_3-Cu water nanofluid in a differentially heated porous cavity

S.A.M. Mehryan [a], Farshad M. Kashkooli [b], Mohammad Ghalambaz [c,*], Ali J. Chamkha [d,e]

[a] Young Researchers and Elite Club, Yasooj Branch, Islamic Azad University, Yasooj, Iran
[b] Department of Mechanical Engineering, K. N. Toosi University of Technology, Tehran, Iran
[c] Department of Mechanical Engineering, Dezful Branch, Islamic Azad University, Dezful, Iran
[d] Mechanical Engineering Department, Prince Mohammad Bin Fahd University, Al-Khobar 31952, Saudi Arabia
[e] Prince Sultan Endowment for Energy and Environment, Prince Mohammad Bin Fahd University, Al-Khobar 31952, Saudi Arabia

ARTICLE INFO

Article history:
Received 13 January 2017
Received in revised form 16 May 2017
Accepted 11 June 2017
Available online 20 June 2017

Keywords:
Hybrid nanofluids
Porous media
Al_2O_3-Cu water
Natural convection

ABSTRACT

Hybrid nanofluids are a new type of enhanced working fluids, engineered with enhanced thermo-physical properties. The hybrid nanofluids profit from the thermo-physical properties of more than one type of nanoparticles. The present study aims to address the free convective heat transfer of the Al_2O_3-Cu water hybrid nanofluid in a cavity filled with a porous medium. Two types of important porous media, glass ball and aluminum metal foam, are considered for the porous matrix. The experimental data show dramatic enhancement in the thermal conductivity and dynamic viscosity of the synthesized hybrid nanofluids, and hence, these thermophysical properties could not be modeled using available models of nanofluids. Thus, the actual available experimental data for the thermal conductivity and the dynamic viscosity of hybrid nanofluids are directly utilized in the present theoretical study. Various comparison with results published previously in the literature are performed and the results are found to be in excellent agreement. In most cases, the average Nusselt number Nu_l is decreasing function of the volume fraction of nanoparticles. The results show the reduction of heat transfer using nanoparticles in porous media. The observed reduction of the heat transfer rate is much higher for hybrid nanofluid compared to the single nanofluid.

1. Introduction

Investigation of the natural convective heat transfer in a porous cavity for its engineering usages, include heat removal in heat exchangers [1] and heat storage systems in solar collectors enhanced with porous matrixes [2,3], and active nuclear west disposal systems [4] has been highly regarded. There are also applications for nanofluids, further than heat transfer such as nanoparticles as anti-microbial agents [5,6] or nanoparticles as radiation absorbent agents [7], in which the heat transfer could be the side advantage or disadvantage of utilizing nanoparticles in the host-fluid. The design of using hybrid nanoparticles as nano-additives can be managed in such applications for multi-purpose benefits including enhancement or inhibition of heat transfer. Thus, the current investigation aims to theoretically study the efficacy of the existence of a hybrid nanofluid in a cavity filled with porous media.

Novel kind of engineered fluids introduced by Choi [8] are the nanofluids that consist of well-dispersed solid nanometer-sized particles [9,10]. Nanoparticles existence in the base-fluid influences significantly its properties. On the other hand, the thermo-physical characteristics of the host-fluid have modified in the presence of nanoparticles. Due to the experimental results, composed nanofluid's density, viscosity, and thermal conductivity are more than the host-fluid's [11]. So, the existence of nanoparticles within the host-fluid affects the convective heat transfer of nanofluid, and is necessary in usages. Neoteric class of nanofluids is hybrid nanofluids which contain a small amount of metal nanoparticles and also non-metallic nanoparticles. Metallic nanoparticles like Zn, Cu, and Al give high thermal conductivities but their use has restrictions such as stability and reactivity. In contrast, non-metallic nanoparticles such as Al_2O_3, CuO, and Fe_3O_4 present lower thermal conductivity in comparison with metallic; however, they have a lot of desirable properties like stability and chemical

* Corresponding author. Fax: +98 (21) 43854961.
E-mail addresses: a.mansuri1366@gmail.com (S.A.M. Mehryan), farshad.moradi@email.kntu.ac.ir (F.M. Kashkooli), m.ghalambaz@iaud.ac.ir (M. Ghalambaz), achamkha@pmu.edu.sa (A.J. Chamkha).

http://dx.doi.org/10.1016/j.apt.2017.06.011
0921-8831/

Nomenclature

Latin symbols

C_p	heat capacity in constant pressure (kJ kg^{-1}K^{-1})
g	gravitational acceleration vector (m s^{-2})
h	local convection coefficient
H	interface heat transfer coefficient parameter
k	thermal conductivity (W m^{-1} K^{-1})
K	permeability of the porous medium (m^2)
L	square cavity size (m)
Nu_x	local Nusselt number
Nu_l	average Nusselt number
p	pressure (Pa)
q''	total interfacial heat flux (W m^{-2})
Ra	Rayleigh number
T	temperature (K)
u, v	velocity components along x, y directions, respectively (m s^{-1})
V	Darcian velocity vector
x, y	Cartesian coordinates (m)

Greek symbols

α	effective thermal diffusivity (m^2 s^{-1})
β	thermal expansion coefficient of the fluid (K^{-1})
ε	porosity of the porous medium
θ	dimensionless temperature
μ	dynamic viscosity (kg m^{-1} s^{-1})
ρ	density (kg m^{-3})
(ρc)	effective heat capacity (J K^{-1} m^{-3})
φ	relative nanoparticle volume fraction
ψ	dimensionless stream function

Subscripts

bf	base-fluid
c	cold
h	hot
hnf	hybrid nanofluid
l	liquid phase
m	effective
max	maximum
nf	nanofluid
r	relative
s	solid porous matrix
x	in x-direction

inertness. Thus, it is hoped that adding Cu to an Al_2O_3-based nanofluid can increase the thermophysical characteristics of the resulting mixture without reducing the nanofluid stability [12,13].

Recently, a lot of experimental studies [12,14–19] and numerical investigations [13,20–25] have been conducted on hybrid nanofluid as a novel technology concept. The thermal conductivity and viscosity of the Al_2O_3–Cu/H_2O hybrid nanofluid have been measured by Suresh et al. [12]. The results demonstrated that both parameters of the hybrid nanofluid enhance with the volume concentrations of nanoparticles. Moghadassi et al. [24] studied the influences of the nanofluid (water-based Al_2O_3) and hybrid nanofluid (Al_2O_3-Cu) and indicated that the hybrid nanofluid has a much larger coefficient of convection heat transfer. Esfe et al. [19] measured the thermal conductivity of SWCNTs-MgO/EG hybrid nanofluids and modeled the experimental data using artificial neural network. Sarkar et al. [26] conducted a comprehensive review briefing recent challenges and investigations in the area of hybrid nanofluids such as heat transfer, synthesis, thermodynamic properties, etc. Tayebi and Chamkha [13] studied numerically the heat transfer in an annulus between two confocal elliptic cylinders filled with Cu-Al_2O_3/water hybrid nanofluid. Three-dimensional hybrid nanofluid boundary-layer flow passing a stretching sheet under the effects of Newtonian heating and Lorentz force has been accomplished by Devi and Anjali [23]. Laminar convective heat transfer of using different base fluids and a hybrid nanofluid in a uniformly heated circular tube is numerically investigated by Takabi et al. [21].

Many researchers have studied experimentally and numerically the influence of the nanofluid on convective heat transfer within enclosures for various conditions and case studies [27–37]. In enclosures, because of no requirement to an exterior power supplies such as electrical source for inducing convective heat transfer, this mechanism of heat transfer is significant. Free convection has some advantages including the decrease of magnetic noise, fee, and sound due to the absence of power sources. These benefits cause the enclosures as an attractive subject for the researchers and various industrials. Baïri et al. [1] have presented a great review on the free convection mechanism in cavities for industrial usages. Most of the time, the cavities are filled by porous media that is saturated with a fluid or a nanofluid. Recent advances in the field of heat transfer and nanofluid flow in a porous medium have been conducted with an excellent review by Kasaeian et al. [38]. Lately, a number of authors have focused on various thermal boundary conditions in cavities. Uniform, non-uniform, and sinusoidal temperature distribution in some or all of the walls and also insulated and adiabatic boundary conditions have used in these problems [39–42]. Use of local thermal equilibrium [43] (when the fluid and solid temperature is equals) and local thermal non-equilibrium (where the fluid and solid temperature is varied) [42,44] models for porous media is another challenging subjects in enclosure filled with nanofluid investigations. Most recently, a number of scholars concentrated on conjugate natural convections in cavities [9,45,46] for its important applications in electrical parts cooling, collectors of solar energy, production of material, etc. Ghalambaz et al. [37] have considered the presence of viscous dissipation and radiation influences on the free convective heat transfer within a square enclosure filled by porous media saturated with nanofluid. Free convection in a differentially heated and partially-layered porous cavity filled by a nanoliquid is examined by Chamkha and Ismael [30]. Al-Zamily [47] conducted a review about the latest progresses in free convection and entropy generation in an enclosure filled by multi-layer porous media, and nanoliquid with considering heat generation. Mansour et al. [33] and Sheremet et al. [35] checked out the influence of the presence of nanoparticles on the magneto-hydrodynamic convection heat transfer of nanofluids in a cavity.

Investigation of using a hybrid nanofluid in cavity problems has newly conducted by some of the researchers [48–50] but to the best of author's knowledge, the free convective heat transfer of hybrid nanofluids in a cavity filled by a porous media has not been addressed yet. As a case study, Al_2O_3-Cu water nanofluid is adopted as a synthesized hybrid nanofluid, as its thermophysical data are available in the literature [12,21,23,24]. The thermal conductivity values of the glass balls and aluminum foam are 1.05 and 205, respectively [27]; hence, the glass balls and aluminum porous foams are adopted as low and high thermal conductive porous matrixes, respectively. The effect of using the hybrid nanofluid on the natural convective behavior of the hybrid nanofluid and the porous media is investigated for the first time to answer the

following questions related to the heat transfer aspect of hybrid nanofluids:

1. Does using hybrid nanofluids assist heat transfer in a cavity filled with a porous media?
2. What is the thermal advantage of using the Al_2O_3-Cu water hybrid nanofluid instead of using a regular Al_2O_3 water nanofluid?
3. What is the influence of the thermal conductivity of the porous medium on the enhancement or deterioration of heat transfer in the cavity by using hybrid nanofluids?
4. Does the increment of the volume fraction of nanoparticles always enhance the heat transfer?
5. Does the increase of the porosity of the porous matrix increase the heat transfer of using the hybrid nanofluid?

With these questions in mind, we now proceed to the next section to present a formulation for natural convective the heat transfer of hybrid nanofluids in a cavity filled with porous media.

2. Basic equations

A cavity filled with a porous medium saturated by a hybrid nanofluid with the size L is depicted in Fig. 1. The top and bottom walls are well insulated, and the left and right walls are kept in the hot and cold temperature of T_h and T_c, respectively. Here, it is assumed that the nanoparticles are always suspended and stable which means that there is no agglomeration and sedimentation (see [51–53]). It is assumed that the interaction of the porous medium and the hybrid nanofluid is high, and hence, the temperature of the porous matrix and the temperature of the hybrid nanofluid are equal throughout the porous medium. Thus, the local thermal equilibrium model is utilized which as a result the temperature can be represented by the effective temperature of T_m. It is assumed that the porous medium is homogeneous and isotropic.

In the present study, it is assumed that the temperature difference is limited. Thus, the results of the present study are valid for the low temperature differences about 10 °C. As the temperature difference is low, it can be assumed that the change in the thermo-physical properties of the materials is limited. However, the presence of nanoparticles would effectively change the thermo-physical properties of the nanofluid and their changes are taken into account. In addition, the change in the density induces a buoyancy force which results in the convective heat transfer flows in the enclosure which is important and should be taken into account. Following [27,29,54], when the temperature difference is low, the buoyancy forces can be represented by the Boussinesq's model. As the size of the porous pores in most of the porous matrices such as aluminum foams or glass balls are small, the flow would quickly reach to its steady state situation and the laminar flow due to the pore walls is reasonable and the flow can be described by the Darcy flow [29–31]. Finally, as the temperature differences in the enclosure is limited and the pores are small, the temperature difference between the solid matrix of the pores and the fluid inside the pores can be neglected [27,29]. Finally, all of the cavity walls are impermeable to both of the base fluid and the nanoparticles.

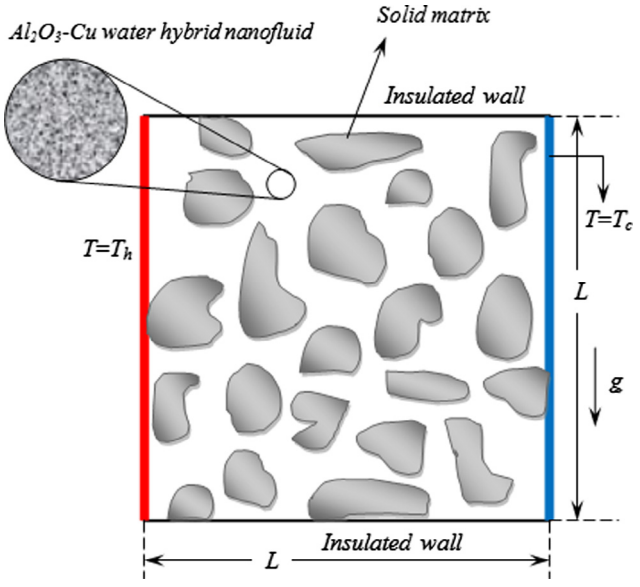

Fig. 1. Schematic of the problem in the present work.

Considering the described assumptions, the governing equations for the hybrid nanofluid can be expressed as [55]:

Continuity equation:

$$\nabla \cdot \mathbf{V} = 0 \tag{1}$$

Momentum equation:

$$0 = -\nabla p - \frac{\mu_{hnf}}{K}\mathbf{V} - (\rho\beta)_{hnf}(T - T_0)\mathbf{g} \tag{2}$$

Energy equation:

$$(\mathbf{V} \cdot \nabla)T_m = \frac{k_{\mathrm{hnf,m}}}{(\rho C_p)_{\mathrm{hnf}}}\left(\frac{\partial^2 T_m}{\partial \bar{x}^2} + \frac{\partial^2 T_m}{\partial \bar{y}^2}\right) \tag{3}$$

where **V**, k, K, p, **g**, β, μ, ρ, and Cp are the Darcian velocity vector; thermal conductivity, permeability of the porous medium, pressure, gravitational acceleration vector, thermal expansion coefficient, dynamic viscosity, density, and the specific heat capacity at a constant pressure, respectively.

The physical properties of the hybrid nanofluid including thermal conductivity k_{hnf}, effective dynamic viscosity μ_{hnf}, buoyancy coefficient $(\rho\beta)_{\mathrm{hnf}}$, and heat capacitance $(\rho C_p)_{\mathrm{hnf}}$ which can be obtained directly from the available experimental data or be calculated from the available expressions presented therein.

At the present time, no accurate models for evaluation of the thermal conductivity and the dynamic viscosity of hybrid nanofluids exist. However, there are some relations which are obtained using curve fitting of the experimental data. Hence, here in order to perform a realistic analysis, we directly utilize the available data for the thermal conductivity and the dynamic viscosity of a hybrid Al_2O_3-Cu water nanofluid. The experimental results for the thermal conductivity and the dynamic viscosity of hybrid Al_2O_3-Cu water nanofluid as a function of various volume fractions of nanoparticles are shown in Table 1. In this table, the experimental values for the thermal conductivity and the dynamic viscosity of regular Al_2O_3/water nanofluid are also provided. The samples of Al_2O_3–Cu hybrid particles have been synthesized by the hydrogen reduction technique from the powder mixture of Al_2O_3 (90%) and CuO (10%). Afterward, Al_2O_3–Cu/water hybrid nanofluids with 0.1–2% volume fractions were prepared by a two-step method: First, a nanofluid with a specified volume concentration was prepared by dispersing a required dose of Al_2O_3–Cu nanoparticles in deionized water with dispersant (Sodium Lauryl Sulphate) using an ultrasonic vibrator producing ultrasonic pulses of 180 W at 40 kHz. Then, the nanofluids were kept under ultrasonic vibration continuously for 6 h to have a stable suspension and uniform dispersion [12].

The relations for evaluation the other thermo-physical properties, such as density, heat capacity, and buoyancy coefficient are summarized in Table 2. These relations are mainly derived from the concentration of mass and energy laws and are mostly in

Table 1
Experimental data for thermal conductivity and dynamic viscosity of hybrid Al_2O_3-Cu/water nanofluid and regular Al_2O_3/water nanofluid.

φ_{hnp} (%)	φ_{Cu} (%)	φ_{Al2O3} (%)	$K_{Al2O3/water}$ (W/m K)	$\mu_{Al2O3/water}$ (kg/m s)	$K_{Al2O3\text{-}Cu/water}$ (W/m K)	$\mu_{Al2O3\text{-}Cu/water}$ (kg/m s)
0.1	0.0038	0.0962	0.614055	0.0009041	0.619982	0.000972
0.33	0.0125	0.3175	0.6190041	0.0009049	0.63098	0.001098
0.75	0.0285	0.7215	0.6309797	0.0009098	0.649004	0.001386
1	0.038	0.962	0.6437496	0.00095184	0.657008	0.001602
2	0.0759	1.9241	0.6571916	0.000972	0.684992	0.001935

Table 2
Applied relations for hybrid nanofluid properties [25].

Hybrid nanofluid properties	Applied relation
Density	$\rho_{hnf} = \rho_f(1-\varphi_{hnp}) + \rho_{Al_2o_3}\varphi_{Al_2o_3} + \rho_{Cu}\varphi_{Cu}$
Buoyancy coefficient	$(\rho\beta)_{hnf} = (1-\varphi_{hnp})(\rho\beta)_f + \varphi_{Al_2o_3}(\rho\beta)_{Al_2o_3} + \varphi_{Cu}(\rho\beta)_{Cu}$
Heat capacity	$(\rho c_p)_{hnf} = (1-\varphi_{hnp})(\rho c_p)_f + \varphi_{Al_2o_3}(\rho c_p)_{Al_2o_3} + \varphi_{Cu}(\rho c_p)_{Cu}$

proper agreement with the experimental results. Following [54], the relations for evaluating the physical properties of a liquid in a saturated porous medium are given by

$$(\rho C_p)_{l,m} = \varepsilon(\rho C_p)_l + (1-\varepsilon)(\rho C_p)_s \tag{4a}$$

$$k_{l,m} = \varepsilon k_l + (1-\varepsilon)k_s, \quad \alpha_{l,m} = \frac{k_{l,m}}{(\rho C_p)_l} \tag{4b}$$

where ε represent the porous media porosity, the indices l, s and m denote the properties associated with the liquid phase (hybrid nanofluid), solid phase (the porous matrix), and effective properties for liquid saturated porous medium, respectively. The above relations are in good agreement with the studies of [29,55] in the case of nanofluids. Indeed, in Eq. (4) the thermo-physical properties of the hybrid nanofluid are coupled with the thermo-physical properties of the porous media. The thermo-physical properties for the host-fluid, nanoparticles and the porous media are demonstrated in Table 3. The glass balls and aluminum foam are two types of common porous media in the literature [27]. As shown in Table 3, the thermal conductivity of the glass balls and aluminum foam are low and high, respectively. Hence, to study the effects of the thermal conductivity of the solid matrix of the porous medium on the flow and heat transfer characteristics, these two types of solid matrix with different thermal conductivities have been adopted.

Eliminating the pressure by cross differentiating between the x and y momentum equations, the governing equations of (1)(3) can be written in Cartesian coordinates as:

$$\frac{\partial \bar{u}}{\partial \bar{x}} + \frac{\partial \bar{v}}{\partial \bar{y}} = 0 \tag{5}$$

$$\frac{\mu_{hnf}}{K}\left(\frac{\partial \bar{u}}{\partial \bar{y}} - \frac{\partial \bar{v}}{\partial \bar{x}}\right) = -g(\rho\beta)_{hnf}\frac{\partial T}{\partial \bar{x}} \tag{6}$$

$$\bar{u}\frac{\partial T}{\partial \bar{x}} + \bar{v}\frac{\partial T}{\partial \bar{y}} = \alpha_{hnf,m}\left(\frac{\partial^2 T}{\partial \bar{x}^2} + \frac{\partial^2 T}{\partial \bar{y}^2}\right) \tag{7}$$

Table 3
Thermophysical properties of the components of Cu-Al_2O_3/water (see [29,32]) and solid structures of the porous media.

Physical properties	Water	Cu	Al_2O_3	Glass balls	Aluminum foam
C_p (J/kg K)	4179	385	765	840	897
k (W/m K)	0.613	401	40	1.05	205
$\alpha \times 10^{-7}$ (m^2/s)	1.47	1163.1	131.7	4.63	846.4
$\beta \times 10^{-5}$ (K^{-1})	21	1.67	0.85	0.9	2.22
ρ (kg/m^3)	997.1	8933	3970	2700	2700
$\mu \times 10^{-4}$ (kg/m s)	8.9	–	–	–	–

Table 4
Grid independency test for the pure fluid when $Ra = 10^3$ and $\varphi_{hnf} = 0$.

Grid size	Nu_l	Error (%)	$\lvert\psi\rvert_{max}$	Error (%)
50 × 50	13.392		20.556	
100 × 100	13.569	1.32	20.510	0.22
150 × 150	13.608	0.28	20.501	0.04
200 × 200	13.622	0.10	20.498	0.01

Table 5
Values calculated for average Nusselt number in a porous triangular shaped enclosure occupied by Cu-water nanofluid.

Ra	***φ***	Sun and pop [31]	Sheremet et al. [29]	Present work
500	0	9.66	9.65	9.64
1000	0.1	9.42	9.41	9.42
500	0	13.9	14.05	13.96
1000	0.2	12.85	12.84	12.85

Using the concept of the stream function as $\bar{u} = \frac{\partial \bar{\psi}}{\partial \bar{y}}$, $\bar{v} = -\frac{\partial \bar{\psi}}{\partial \bar{x}}$ and invoking the following non-dimensional parameters:

$$x = \bar{x}/L, \quad y = \bar{y}/L, \quad \psi = \bar{\psi}/\alpha_{b,m}, \quad \theta = (T-T_c)/(T_h-T_c) \tag{8}$$

The non-dimensional form of the governing equations is gained as:

$$\frac{\partial^2 \psi}{\partial x^2} + \frac{\partial^2 \psi}{\partial y^2} = -Ra.H.\frac{\partial \theta}{\partial x} \tag{9}$$

$$\frac{\partial \psi}{\partial y}\frac{\partial \theta}{\partial x} - \frac{\partial \psi}{\partial x}\frac{\partial \theta}{\partial y} = \alpha_r\left(\frac{\partial^2 \theta}{\partial x^2} + \frac{\partial^2 \theta}{\partial y^2}\right) \tag{10}$$

The boundary conditions can be written as below:

$$\begin{aligned} &\psi = 0, \quad \theta = 1 \quad \text{on} \quad x = 0 \\ &\psi = 0, \quad \theta = 0 \quad \text{on} \quad x = 1 \\ &\psi = 0, \quad \tfrac{\partial \theta}{\partial y} = 0 \quad \text{on} \quad y = 0 \\ &\psi = 0, \quad \tfrac{\partial \theta}{\partial y} = 0 \quad \text{on} \quad y = 1 \end{aligned} \tag{11}$$

Here in this specific problem, the Rayleigh number is the Darcy-Rayleigh number, introduced due to the thermo-physical properties of the host fluid and the porous medium as $Ra = gK(\rho\beta)_{bf}(T_h - T_c)L/(\alpha_{bf,m}\mu_{bf})$, $H = \left(\frac{(\rho\beta)_{hnf}}{(\rho\beta)_{bf}}\right)\left(\frac{\mu_{bf}}{\mu_{hnf}}\right)$ and $\alpha_r = \left(\frac{\alpha_{hnf,m}}{\alpha_{bf,m}}\right)$. The thermo-physical properties for the hybrid nanofluid and the base fluid can be evaluated using Tables 1–3 and the coupling relations introduced in Eq. (4).

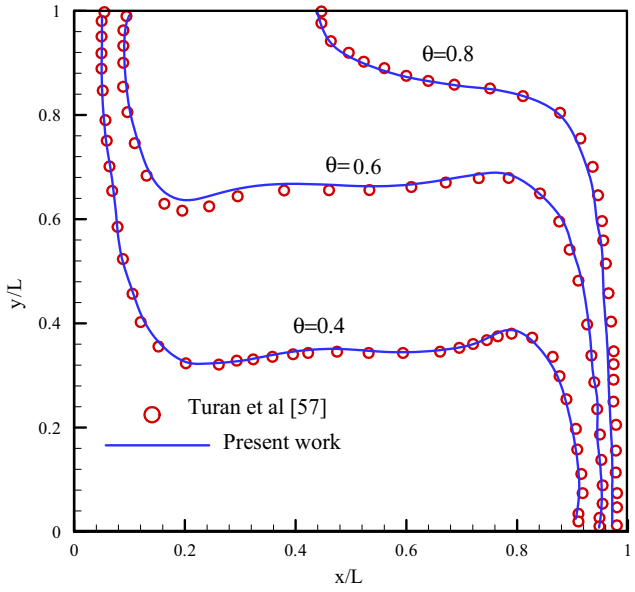

Fig. 2. Isotherms concluded by this work (lines) and Turan et al. [60] (circular points).

The rate of heat transfer in the cavity can be evaluated at the surface of one of the vertical isotherms walls of the cavity. For instance, The conduction heat transfer at the left isotherm wall can be written as $q'' = k_{hnf,m}\left(\frac{\partial \bar{T}}{\partial \bar{x}}\right)_{\bar{x}=0}$. The convection heat transfer at the left wall can be evaluated using $q'' = h_x(T_h - T_c)$ where h_x is the local convection coefficient. Based on the conservation equation of energy, the conduction heat transfer at the wall is equal to the convection heat transfer which yields $k_{hnf,m}\left(\frac{\partial \bar{T}}{\partial \bar{x}}\right)_{\bar{x}=0} = h_x(T_h - T_c)$ where invoking the non-dimensional variables gives:

$$\frac{h_x L}{k_{bf,m}} = -\frac{k_{hnf,m}}{k_{bf,m}}\left(\frac{\partial \theta}{\partial x}\right)_{x=0} \tag{12}$$

By introducing the local Nusselt number due to the effective thermal conductivity of the base fluid and the porous media as $Nu_x = \frac{h_x L}{k_{bf,m}}$, Eq. (12) is written as:

$$Nu_x = -\frac{k_{hnf,m}}{k_{bf,m}}\left(\frac{\partial \theta}{\partial x}\right)_{x=0} \tag{13}$$

and the average Nusselt numbers at the left wall is calculated as below:

$$Nu_l = \frac{1}{L}\int_0^L Nu_x\, dy \tag{14}$$

In a similar way, the local Nusselt number and the average Nusselt number can be introduced for the right wall.

3. Numerical method

A two-equation system including partial differential Eqs. (9) and (10), based on the above-mentioned boundary conditions, is

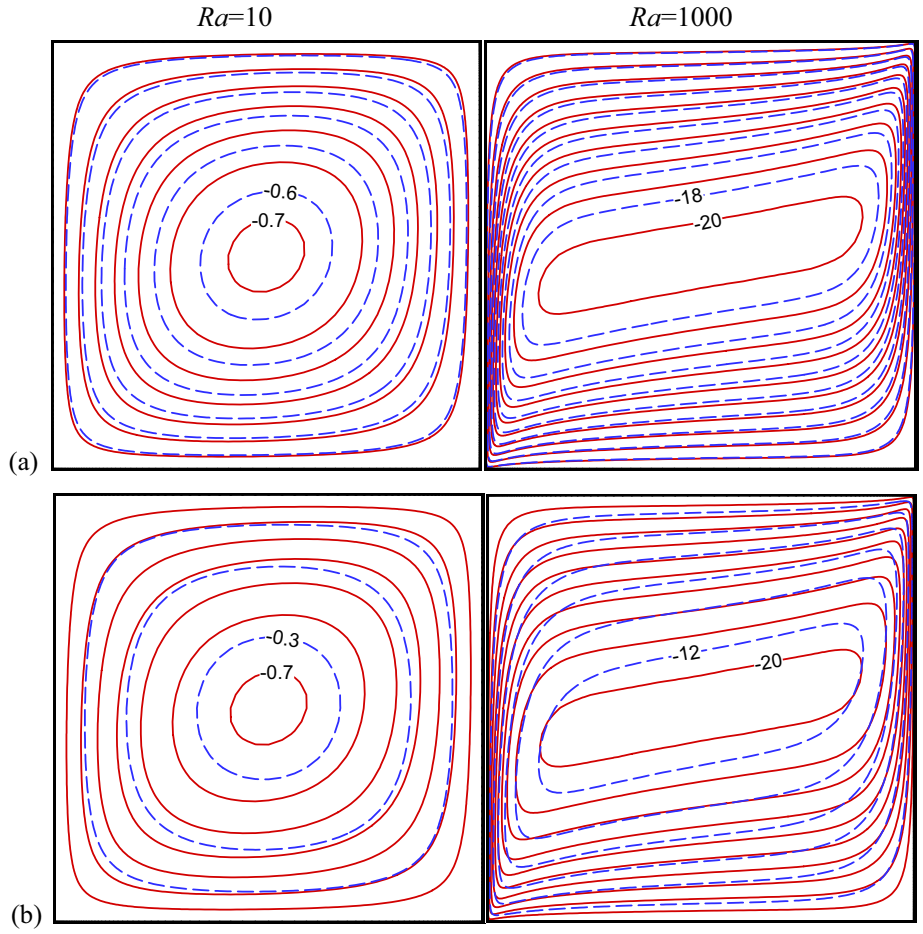

Fig. 3. streamlines for pure fluid (solid lines), (a): Al_2O_3 nanofluid (dash lines) (b): Cu-Al_2O_3 hybrid nanofluid (dash lines) at glass balls porous medium for low and high values of Ra = 10 and 1000, respectively, when ε = 0.6 and $\varphi_{hnf} = \varphi_{Al2O3}$ = 0.02.

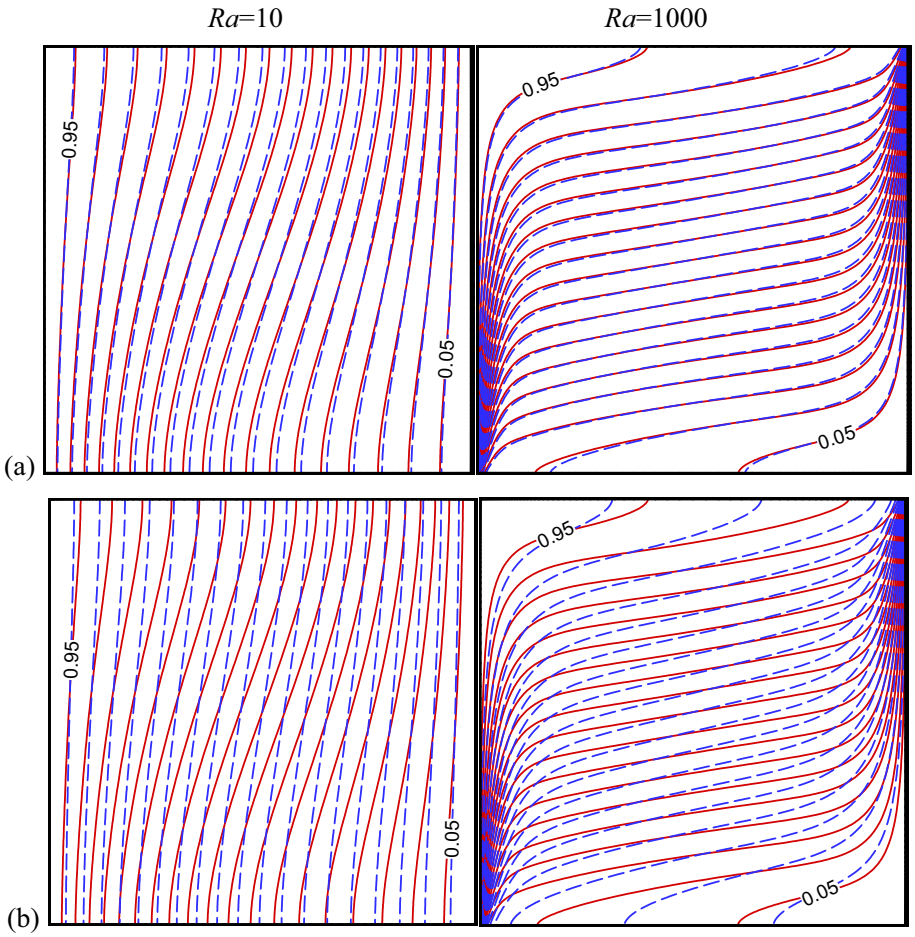

Fig. 4. Isotherms for low and high values of $Ra = 10$ and 1000, respectively, when $\varepsilon = 0.6$ and $\varphi_{hnf} = \varphi_{Al2O3} = 0.02$ and the glass balls are solid matrix of porous medium; (a): Al_2O_3 nanofluid (dash lines) and pure fluid (solid lines) (b): Cu-Al_2O_3 hybrid nanofluid (dash lines) and pure.

converted to the simplified form and solved using the Galerkin weighted residual finite element numerical method [56–58]. A non-uniform structured grid is utilized.

Basically, to accurately simulate the boundary layers formed in the vicinity of the solid boundaries including thermal and hydrodynamics boundaries, the use of a finer mesh in the vicinity of the solid walls is inevitable. Using a finer unstructured mesh next to the walls would effectively capture the important temperature gradients in the vicinity of the walls. However, in the main regions of the enclosure in which the gradients are small, a coarse mesh is also adequate. Hence, using an unstructured grid provides the advantage of an accurate solution with low-cost computations. Hence, a non-uniform structured grid can satisfy these requirements. However, implementing the numerical procedure in a non-uniform mesh is harder than a uniform mesh. Here, the computer solution codes with user-defined functions which are based on the finite element method are utilized for the numerical calculations.

In order to evaluate the residuals, the Biquadratic equation and the three-point Gaussian quadrature formula are employed and to solve them, the Newton–Raphson iteration method is used. When the error is lower than 10^{-7}, the computations are stopped. A detailed discretization of the governing equations and the numerical method has been explained completely in the paper published by Donea and Huerta [59]. The grid independency test is carried out to ensure the accuracy of the solution. In this evaluation, $Ra = 10^3$ and $\varphi_{hnf} = 0$. As shown in Table 4, when the grid size is 100×100, the error percentage of mesh size is much less than 1%, exactly 0.28 and 0.04% for Nu_l and $|\psi|_{max}$, respectively. Hence, the grid size 100×100 is confidently applied to discretize the computational domain.

Reliability of the outcomes of the present work is assessed by re-calculating consequences reported by Sun and pop [31] as well as Sheremet et al. [29] for the natural convection within an enclosed porous medium by the sides of a triangular. The pores are occupied with a Cu-water nanofluid and a heating element was located on the vertical wall of the triangular. The data represented in Table 5 illustrate this validation. Also, the used code is evaluated with the study performed by Turan et al. [60] represented in Fig. 2 that belong to a square enclosure containing pure fluid. The excellent matching between the results of re-calculations of this study and initial papers ensures the accuracy of our results.

4. Results and discussion

Current research studies the free convective heat transfer of a Cu-Al_2O_3/water hybrid nanofluid and also, Al_2O_3/water nanofluid within a porous cavity which its solid matrix is glass balls or aluminum foam. Various values of the Darcy-Rayleigh number ($Ra = 1$–10^3), hybrid volume fraction ($\varphi = 0$–0.02) and porosity ($\varepsilon = 0.3$–0.9) are considered to do calculations for two different kinds of porous media material including glass balls and aluminum foam.

The effect of the presence of the Cu-Al_2O_3 hybrid and Al_2O_3 nanoparticles on the streamlines patterns for low and high values of the Rayleigh number Ra in the porous medium with glass balls solid matrix is illustrated in Fig. 3. When Ra is low ($Ra = 10$),

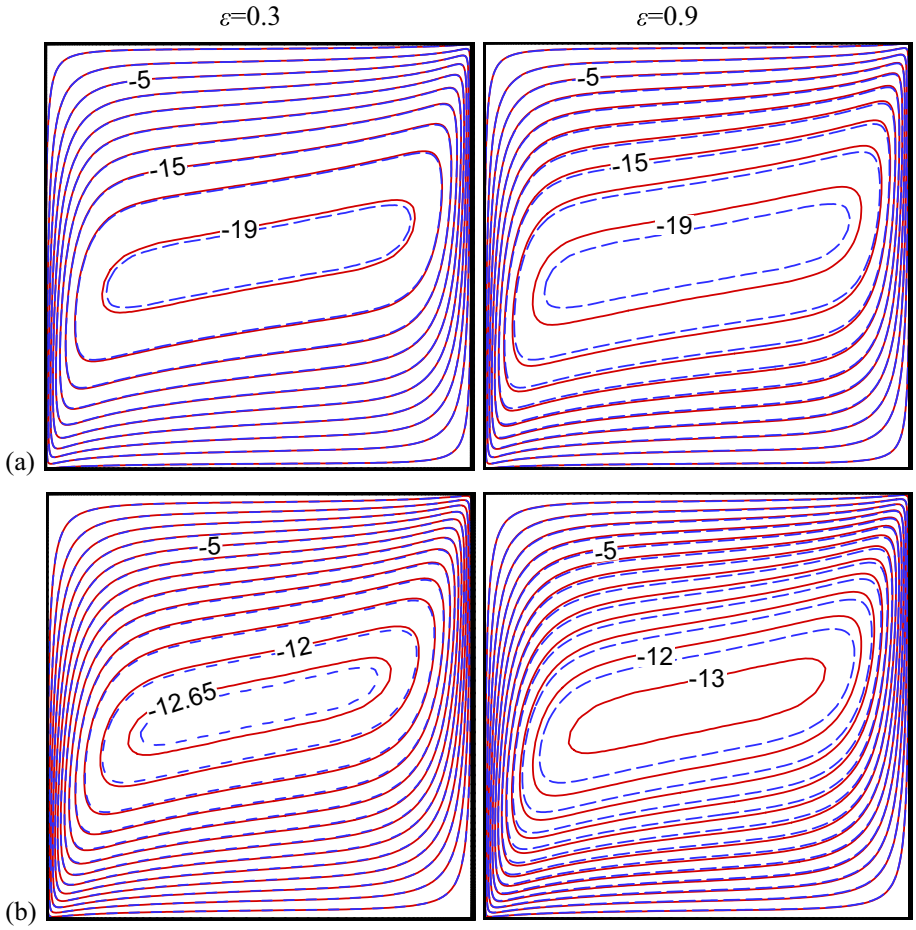

Fig. 5. Streamlines within porous medium with glass balls (solid lines) and Aluminum foam solid matrixes for (a): Al_2O_3/water nanofluid and (b): Cu-Al_2O_3/water hybrid nanofluid at various values of ε when $Ra = 1000$.

regardless of the type of the fluid occupying the porous medium, a weak clockwise recirculating cell is formed within the porous cavity.

For both types of nanoparticles, Cu-Al_2O_3 hybrid and Al_2O_3 nanoparticles, as the Rayleigh number enhances from 10 to 1000, the nanofluid velocity within the square cavity extremely augments. As a result of this increase, the streamlines patterns reshape, so that the circular streamlines formed at $Ra = 10$ are stretched along the horizontal surfaces when $Ra = 1000$. Indeed, the change in the patterns tell us that the convection mode becomes dominant compared to the conduction mode with increasing values of *Ra*. Moreover, it is seen that using both types of the nanoparticles decline the strength of the nanofluid flow for all values of *Ra*. Solid and dash lines correspond to pure and nanofluid, respectively. The reduction of the nanofluid velocity resulting from utilizing Cu-Al_2O_3 hybrid nanoparticles is much more than that of Al_2O_3 nanoparticles. The decline can be attributed to an increase in the dynamic viscosity coming from the presence of the nanoparticles. The experimental data in Table 1 show that simultaneous application of Cu and Al_2O_3 nanoparticles strongly raise the dynamic viscosity of the base fluid. This increment for $\varphi_{hnf} = 0.02$ is 117.4%. Hence, the very drastic increment of the fluid resistance against the buoyancy force is not unexpected when $\varphi_{hnf} = 0.02$.

The corresponding isotherms to the streamlines presented in Fig. 3 are also displayed in Fig. 4. In general, it can be said that the lines of the isotherms' contours are parallel to the vertical boundaries when *Ra* is low ($Ra = 10$) and tend to be formed along the horizontal boundaries at $Ra = 1000$. In fact, at $Ra = 1000$, the convection mechanism is predominated as a heat transfer process; it creates a stratified temperature field with various levels.

The reduction of the thermal boundary layer thickness is obviously observed when *Ra* augments from $Ra = 10$–1000. Compression of the lines of isotherms close to the hot and cold walls in the left-down and right-up regions of the cavity, respectively, illustrates this fact. Furthermore, it is observed that utilizing nanoparticles displaces the isotherms. Indeed, the use of nanoparticles leads to decreases of isotherms stretching along the horizontal surfaces. This means that the contribution of conduction mechanism of heat transfer becomes more comparable to convection as a result of reducing the flow strength. Reducing the isotherms stretching for the hybrid nanofluid is much more than that for the Al_2O_3 nanofluid.

To investigate the influences of the solid material of the porous media on the velocity and temperature fields, the results for the isotherms and the streamlines are presented in Fig. 5 for two types of solid matrices at two values of $\varepsilon = 0.3$ and 0.9. In this detailed study, *Ra* and φ remains constant at 1000 and 0.02, respectively. For a certain case, comparison of the streamlines between cavities containing glass balls and aluminum foam illustrates that the strength of the formed recirculating cells in the cavity containing glass balls is more comparable to the other material of the solid matrix. To justify this result, it should be related to the thermal diffusion ratio α_r, because the other dimensionless parameters remain constant when only the solid matrix material is changed.

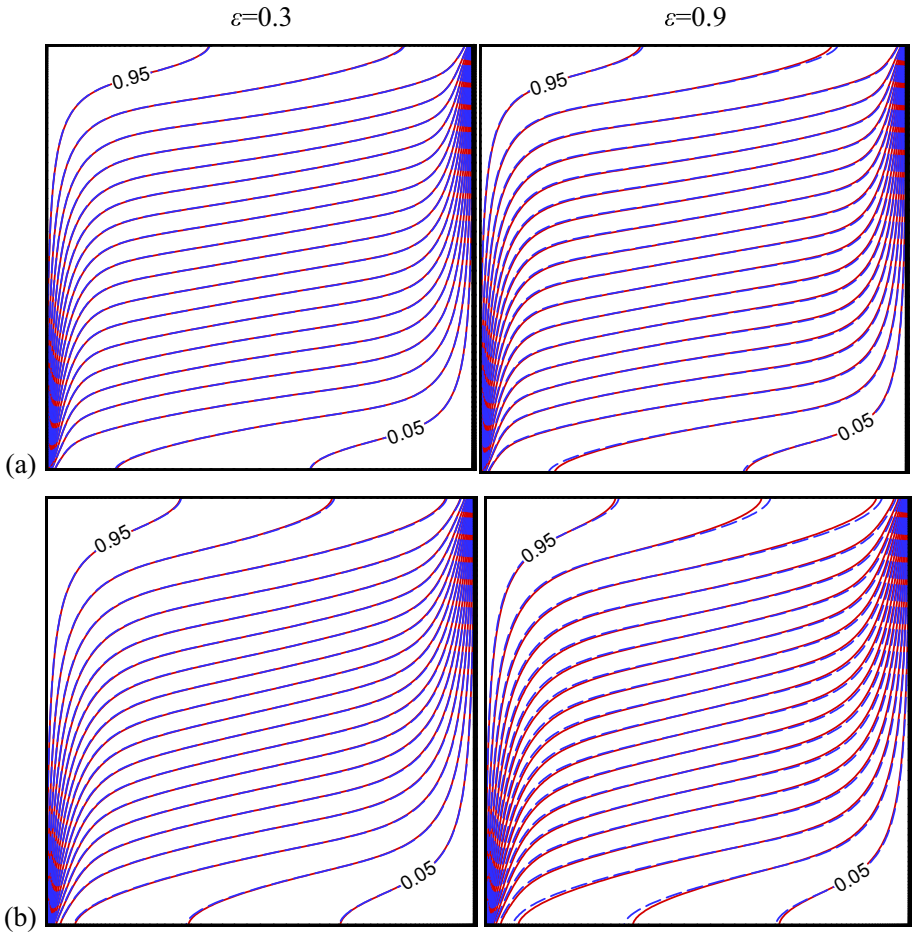

Fig. 6. Isotherms within porous medium with glass balls (solid lines) and Aluminum foam solid matrixes for (a): Al_2O_3/water nanofluid and (b): Cu-Al_2O_3/water hybrid nanofluid at various values of ε when *Ra* = 1000.

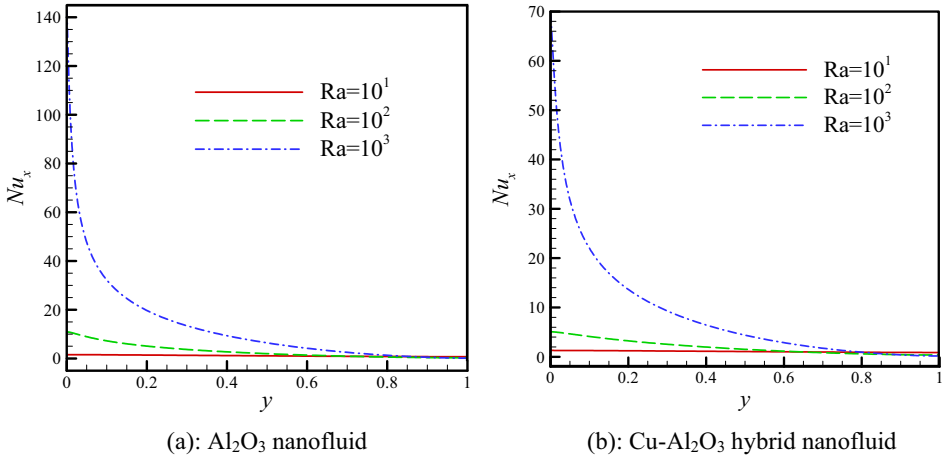

Fig. 7. Local Nusselt number along y axis on the hot boundary Nu_x for (a): Al_2O_3 nanofluid and (b): Cu-Al_2O_3 hybrid nanofluid for porous medium with glass balls solid matrix at various values of Ra and constant values of $\varepsilon = 0.6$ and $\varphi_{Al2O3} = \varphi_{hnf} = 0.02$.

The defined relations for the thermal diffusion ratio α_r tell us that this ratio is more than 1 and decreasingly tends to 1 with the increase in the thermal conductivity of the solid matrix. Hence, it is clear that the thermal diffusion ratio for α_r a medium containing glass balls is more than that for a medium consisting of aluminum foam. On the other hand, we know well that the increment of this ratio boosts the ability of the nanofluid in carrying heat. It is expected that increasing the porosity makes the fluid motion becomes easier because of increasing void spaces. This expectation has been actualized as shown in Fig. 5(a) and (b). Moreover, it is necessary to say that the thermal conductivity effect of the solid matrix on the flow becomes more when the porosity enhances. Fig. 6(a) and (b) show the corresponding isotherms to the streamlines presented in Fig. 5. As demonstrated, there are

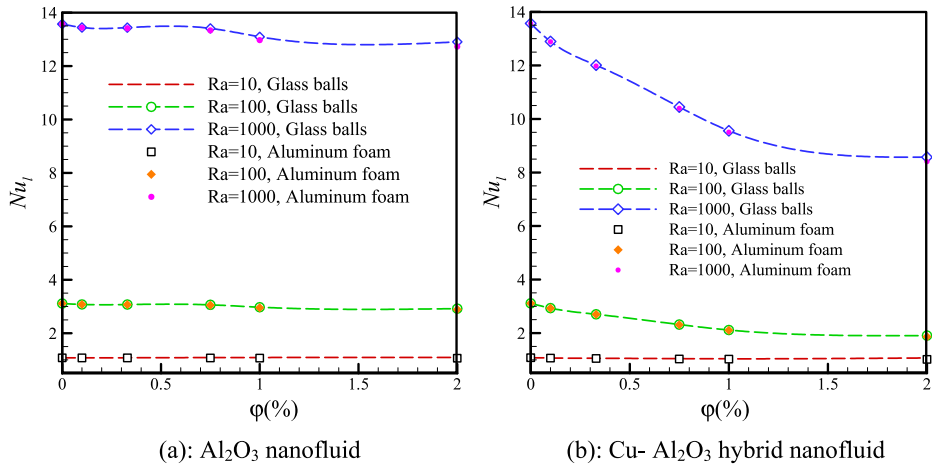

Fig. 8. Variations of the average Nusselt number Nu_l according to volume fraction at various values of *Ra* for both types of glass balls and Aluminum foam solid matrix for (a): Al_2O_3 nanofluid and (b): Cu-Al_2O_3 hybrid nanofluid when $\varepsilon = 0.6$.

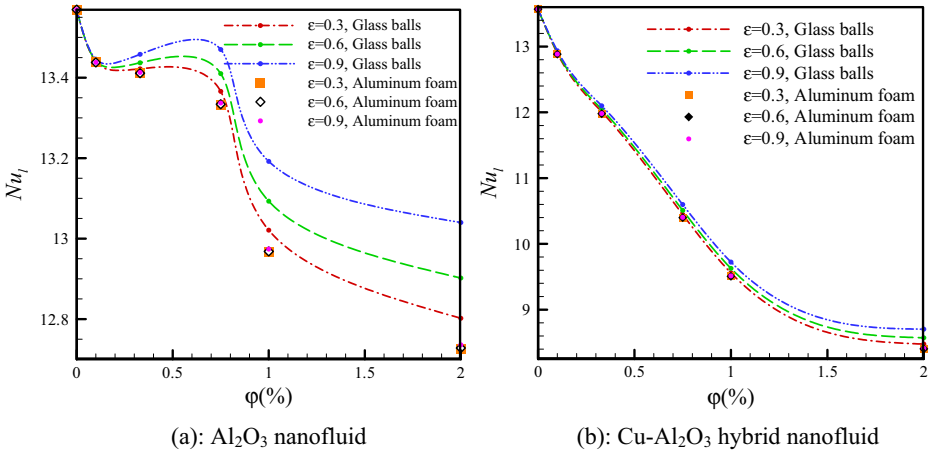

Fig. 9. Influence of the volume fraction on the average Nusselt number at various values of porosity for different types of porous medium solid matrix when *Ra* = 1000.

Table 6
Comparison of the percentage of decrease of the average Nusselt number Nu_l for both types of nanofluid with respect to pure fluid for glass balls solid matrix when *Ra* = 1000 and $\varepsilon = 0.6$.

φ (%)	H_{Al2O3}	$H_{Cu\text{-}Al2O3}$	α_{r_Al2O3}	$\alpha_{r\_Cu\text{-}Al2O3}$	$Nu_{l,\ Al2O3}$	P.R. (%)	$Nu_{l,\ Cu\text{-}Al2O3}$	P.R. (%)
0	1	1	1	1	13.569	0	13.569	0
0.1	0.98358	0.91489	1.0006	1.0056	13.442	0. 94	12.913	5.08
0.33	0.98081	0.80838	1.0055	1.0068	13.437	0. 98	12.046	12.64
0.75	0.97208	0.63820	1.0158	1.0138	13.409	1.19	10.510	29.10
1	0.92719	0.55101	1.0262	1.0171	13.093	3.63	9.6286	40.92
2	0.90028	0.45242	1.0393	1.0290	12.902	5.16	8.5726	58.28

no significant variations in the thermal field when the solid matrix material and the porosity change.

The graphs illustrated in Fig. 7(a) and (b) demonstrate variations trend of the local Nusselt number on the left hot boundary along the y-axis Nu_x for both types of nanofluids at three different values of *Ra* = 10, 100, 1000 when the values of φ and ε are 0.02 and 0.6, respectively. Here, the solid matrix of the porous medium is glass balls. The drastic increment of the local Nusselt number at the beginning of the hot bound, close to the insulated bottom wall, is observed when *Ra* reaches 1000. The very thin thermal boundary layer in this region has the lowest thermal resistance against heat transfer, so the maximum heat transfer rate locally occurs at the lowest part of the hot boundary.

It is interesting to note that the local Nusselt number at the end of the hot wall close to the top wall decreases with the increase of Ra. A close inspection of the figures shows this behavior obviously.

Fig. 8(a) and (b) demonstrate the influences of the volume fraction, Rayleigh number and the solid matrix material of the porous medium on the average Nusselt number of Al_2O_3 and Cu-Al_2O_3 hybrid nanofluids, respectively. As obviously shown, for all the cases, increasing the buoyancy force coming from increasing *Ra* boosts average Nusselt number Nu_l on the hot left boundary. Furthermore, we can see that the reduction of Nu_l by increasing the nanoparticles becomes more at high values of *Ra*. Also, it is worth saying that when *Ra* = 10, the dependence of Nu_l on the volume fraction is low so that it can be confidently ignored. Moreover,

the dependence of Nu_l on the solid matrix material is more prominent at the high values of Ra (Ra = 1000) and φ ($\varphi_{Al2O3} = \varphi_{hnf} = 0.02$). The results show that the Nusselt number of aluminum foam is lower than that of the glass balls. This conclusion does not mean that the heat transfer ability of the aluminum foam porous medium is lower than that of the glass ball porous medium. These results indicate that the utilization of nanoparticles in a glass ball porous medium produces a better heat transfer potential compared to the aluminum foam porous medium. This is due to the fact that the heat transfer ability of the aluminum foam porous medium is much higher than that of the glass ball porous medium. Hence, utilizing of a nanofluid in the aluminum foam porous medium is not much effective, but the effectiveness of using the nanofluid in the glass ball porous medium with low thermal conductivity is more obvious.

To investigate the variations trend of the average Nusselt number with the volume fraction for various porosities for both types of the porous medium solid matrix, the graphs presented in Fig. 9 have been provided. For both types of the solid matrix and all the values of the porosity, expect for glass balls solid matrix when $\varepsilon = 0.9$, there is a decreasing trend with the increase of the volume fraction. At $\varepsilon = 0.9$, when glass balls are used as a solid matrix of the porous media, using Al_2O_3 nanoparticles with $\varphi = 0.1\%$ declines the heat transfer rate. After that, the increment of the nanoparticles up to 0.75% raises the average Nusselt number. Then, a decreasing trend can be observed again when the volume fraction increases. When the solid matrix material of the porous media is the aluminum foam with high thermal conductivity, the average Nusselt number Nu_l is not dependent on the porosity. However, when the solid matrix is the glass balls with low thermal conductivity, the variations of Nu_l with the porosity is considerable. In fact, when the thermal conductivity of the solid matrix is much higher than that for the fluid phase, the thermal diffusion ratio α_r remains almost constant with varying porosity values. This means that the effective thermal conductivity of the porous medium is kept constant. In contrast, for the solid and fluid phases with thermal conductivities close to each other, variations of the porosity can vary the thermal diffusion ratio considerably. Therefore, the nanofluid ability for carrying heat can increases with increasing ε.

Finally, to find out the exact decreasing of the heat transfer rate arising from using Al_2O_3 nanoparticles and also, Cu and Al_2O_3 nanoparticles simultaneously, the values of the average Nusselt number for both types of nanofluids at various values of φ as well as the percentage of their reduction are presented in Table 6. Display and comparison of the dimensionless parameter of H for Al_2O_3 nanofluid and Cu- Al_2O_3 hybrid nanofluid imparts that the reduction of H for hybrid nanoparticles is much more intense than that for Al_2O_3 nanoparticles so that for $\varphi = 0.02$, the value of H for the hybrid nanofluid is half of that for Al_2O_3 nanofluid. However, the values of the thermal diffusion ratios of these nanofluids are very close to each other at a certain volume fraction. For these reasons, the percentage of reduction of the heat transfer rate ($P.R$ contraction used in Table 6) for the Cu-Al_2O_3 hybrid nanofluid is more than tenfold the reduction of the Al_2O_3 nanofluid at $\varphi = 0.02$.

5. Conclusion

The present study investigates free convective heat transfer of Al_2O_3/water nanofluid and Cu-Al_2O_3/water hybrid nanofluid within a square porous cavity. The vertical walls of the cavity are isothermal while the top and bottom walls are insulated. The governing differential equations are obtained using the Darcy model and then for better representation of the results, converted into a non-dimensional form. The finite element method is applied to solve the governing equations. Different values of the Darcy-Rayleigh number ($Ra = 1–10^3$), hybrid volume fraction ($\varphi = 0–0.02$) and the porosity ($\varepsilon = 0.3–0.9$) are examined to perform calculations for two types of porous medium materials; glass balls and aluminum foam. The main findings of the current investigation are as follows:

- The presence of the Cu-Al_2O_3 hybrid and Al_2O_3 nanoparticles causes the nanofluid velocity to extremely increase as Ra enhances, and the strength of nanofluid flow to decrease for all values of Ra.
- The reduction of the nanofluid velocity resulting from utilizing Cu-Al_2O_3 hybrid nanoparticles is much more than that for Al_2O_3 nanoparticles. Besides, a reduction of the thermal boundary layer thickness is observed when Ra augments from $Ra = 10–10^3$.
- Using of the glass balls porous medium in comparison to the aluminum foam increases the strength of the formed recirculating cells. Also, when the porosity enhances, the thermal conductivity effect of the each of the solid matrices increases. Alternating the solid matrix with other type and changing the porosity have no considerable variations in the thermal field inside the cavity.
- When $Ra = 10$, the dependence of the Nu_l on the volume fraction is very low, whereas the dependence of Nu_l on the solid matrix is more prominent at the high values of Ra ($Ra = 10^3$) and φ ($\varphi_{Al2O3} = \varphi_{hnf} = 0.02$).
- For both solid matrices and all the values of porosity, expect for glass balls solid matrix when $\varepsilon = 0.9$, the average Nusselt number has a decreasing trend with the increment of the volume fraction.
- When the solid matrix material is the aluminum foam (with high thermal conductivity), Nu_l is not dependent on the porosity, whereas, when the solid matrix is the glass balls (with low thermal conductivity), the variations of Nu_l with the porosity is considerable.
- The reduction percentage of the heat transfer rate for a hybrid nanofluid is much more than that for a single regular nanofluid.

Acknowledgements

S.A.M. Mehryan is grateful to the Young Researchers and Elite Club, Yasooj Branch, Islamic Azad University, Yasooj, Iran for its financial support. M. Ghalambaz acknowledges the financial support of Dezful Branch, Islamic Azad University, Dezful, Iran. M. Ghalambaz highly appreciates the generous support of dear Mehrnaz. The first, second and third authors are tankful to Iran Nanotechnology Initiative Council (INIC) for the support of the present study.

References

[1] A. Baïri, E. Zarco-Pernia, J.M. García de María, A review on natural convection in enclosures for engineering applications. The particular case of the parallelogrammic diode cavity, Appl. Therm. Eng. 63 (2014) 304–322.
[2] H. Tyagi, P. Phelan, R. Prasher, Predicted efficiency of a low-temperature nanofluid-based direct absorption solar collector, J. Sol. Energy Eng. 131 (2009) 410041–410047.
[3] O. Mahian, A. Kianifar, S.A. Kalogirou, I. Pop, S. Wongwises, A review of the applications of nanofluids in solar energy, Int. J. Heat Mass Transf. 57 (2013) 582–594.
[4] H. Tyagi, Radiative and combustion properties of nanoparticle-laden liquids, Arizona State University, 2008.
[5] L. Zhang, Y. Ding, M. Povey, D. York, ZnO nanofluids–a potential antibacterial agent, Prog. Nat. Sci. 18 (2008) 939–944.
[6] K. Hirota, M. Sugimoto, M. Kato, K. Tsukagoshi, T. Tanigawa, H. Sugimoto, Preparation of zinc oxide ceramics with a sustainable antibacterial activity under dark conditions, Ceram. Int. 36 (2010) 497–506.
[7] J.F. Dorsey, L. Sun, D.Y. Joh, A. Witztum, G.D. Kao, M. Alonso-Basanta, S. Avery, S.M. Hahn, Gold nanoparticles in radiation research: potential applications for imaging and radiosensitization, Transl. Cancer Res. 2 (2013) 280–291.

[8] S.U.S. Choi, J.A. Eastman, Enhancing thermal conductivity of fluids with nanoparticle, in: D.A. Siginer, H.P. Wang (Eds.), Developments and applications of non-Newtonian flows, FED vol. 231 and MD vol. 66. ASME; (1995) 99–105.

[9] A.J. Chamkha, M.A. Ismael, Conjugate heat transfer in a porous cavity filled with nanofluids and heated by a triangular thick wall, Int. J. Therm. Sci. 67 (2013) 135–151.

[10] S.A.M. Mehryan, F. Moradi Kashkooli, M. Soltani, K. Raahemifar, Fluid flow and heat transfer analysis of a nanofluid containing motile gyrotactic microorganisms passing a nonlinear stretching vertical sheet in the presence of a non-uniform magnetic field; numerical approach, PLOS ONE 11 (2016) e0157598, http://dx.doi.org/10.1371/journal.pone.0157598.

[11] S. Kakaç, A. Pramuanjaroenkij, Review of convective heat transfer enhancement with nanofluids, Int. J. Heat Mass Transf. 52 (2009) 3187–3196.

[12] S. Suresh, K. Venkitaraj, P. Selvakumar, M. Chandrasekar, Synthesis of Al_2O_3–Cu/water hybrid nanofluids using two step method and its thermo physical properties, Colloids Surf. A 388 (2011) 41–48.

[13] T. Tayebi, A.J. Chamkha, Free convection enhancement in an annulus between horizontal confocal elliptical cylinders using hybrid nanofluids, Numer. Heat Transf., Part A: Appl. 70 (2016) 1141–1156, http://dx.doi.org/10.1080/10407782.2016.1230423.

[14] D. Madhesh, R. Parameshwaran, S. Kalaiselvam, Experimental investigation on convective heat transfer and rheological characteristics of Cu–TiO_2 hybrid nanofluids, Exp. Therm. Fluid Sci. 52 (2014) 104–115.

[15] M. Afrand, D. Toghraie, N. Sina, Experimental study on thermal conductivity of water-based Fe_3O_4 nanofluid: development of a new correlation and modeled by artificial neural network, Int. Commun. Heat Mass Transfer 75 (2016) 262–269.

[16] P. Jena, E. Brocchi, M. Motta, In-situ formation of Cu–Al_2O_3 nano-scale composites by chemical routes and studies on their microstructures, Mater. Sci. Eng., A 313 (2001) 180–186.

[17] M.J. Nine, M. Batmunkh, J.H. Kim, H.S. Chung, H.M. Jeong, Investigation of Al_2O_3-MWCNTs hybrid dispersion in Water and their thermal characterization, J. Nanosci. Nanotechnol. 12 (2012) 4553–4559.

[18] M.J. Nine, B. Munkhbayar, M.S. Rahman, H. Chung, H. Jeong, Highly productive synthesis process of well dispersed Cu_2O and Cu/Cu_2O nanoparticles and its thermal characterization, Mater. Chem. Phys. 141 (2013) 636–642.

[19] M.H. Esfe, S.H. Rostamian, A. Alirezaie, An applicable study on the thermal conductivity of SWCNT-MgO hybrid nanofluid and price-performance analysis for energy management, Appl. Therm. Eng. 111 (2017) 1202–1210.

[20] T. Takabi, S. Salehi, Augmentation of the heat transfer performance of a sinusoidal corrugated enclosure by employing hybrid nanofluid, Adv. Mech. Eng. 6 (2014) 147059.

[21] B. Takabi, A.M. Gheitaghy, P. Tazraei, Hybrid Water-based suspension of Al_2O_3 and Cu nanoparticles on laminar convection effectiveness, J. Thermophys. Heat Transf. 30 (2016) 523–532.

[22] R. Nasrin, M. Alim, Finite element simulation of forced convection in a flat plate solar collector: influence of nanofluid with double nanoparticles, J. Appl. Fluid Mech. 7 (2014) 543–556.

[23] S.S.U. Devi, S.A. Devi, Numerical investigation of three-dimensional hybrid Cu–Al_2O_3/water nanofluid flow over a stretching sheet with effecting Lorentz force subject to newtonian heating, Can. J. Phys. 94 (2016) 490–496.

[24] A. Moghadassi, E. Ghomi, F. Parvizian, A numerical study of water based Al_2O_3 and Al_2O_3-Cu hybrid nanofluid effect on forced convective heat transfer, Int. J. Therm. Sci. 92 (2015) 50–57.

[25] R. Nimmagadda, K. Venkatasubbaiah, Conjugate heat transfer analysis of micro-channel using novel hybrid nanofluids Al_2O_3+Ag/water, Eur. J. Mech. B/Fluids 52 (2015) 19–27.

[26] J. Sarkar, P. Ghosh, A. Adil, A review on hybrid nanofluids: Recent research, development and applications, Renew. Sustain. Energy Rev. 43 (2015) 164–177.

[27] M. Ghalambaz, M.A. Sheremet, I. Pop, Free convection in a parallelogrammic porous cavity filled with a nanofluid using Tiwari and Das' nanofluid model, PLOSE ONE 10 (2015) e0126486, http://dx.doi.org/10.1371/journal.pone.0126486.

[28] A.M. Rashad, M.M. Rashidi, Giulio Lorenzini, S. E. Ahmed, A. M. Aly, Magnetic field and internal heat generation effects on the free convection in a rectangular cavity filled with a porous medium saturated with Cu–water nanofluid, Int. J. Heat Mass Transf. 104 (2017) 878–889.

[29] M.A. Sheremet, T. Grosan, I. Pop, Free convection in a square cavity filled with a porous medium saturated by nanofluid using Tiwari and Das' nanofluid model, Transp. Porous Media 106 (2015) (2015) 595–610.

[30] A.J. Chamkha, M.A. Ismael, Natural convection in differentially heated partially porous layered cavities filled with nanofluid, Numer. Heat Transfer, Part A 65 (2014) 1089–1113.

[31] Q. Sun, I. Pop, Free convection in a triangle cavity filled with a porous medium saturated with nanofluids with flush mounted heater on the wall, Int. J. Therm. Sci. 50 (2011) 2141–2153.

[32] E. Abu-Nada, H.F. Oztop, Effects of inclination angle on natural convection in enclosures filled with Cu–water nanofluid, Int. J. Heat Fluid Flow 30 (2009) 669–678.

[33] M.A. Mansour, A.J. Chamkha, M.A.Y. Bakier, Magnetohydrodynamic natural convection and entropy generation of a Cu-Water nanofluid in a cavity with wall mounted Heat source/sink, J. Nanofluids 4 (2015) 254–269.

[34] M.A. Sheremet, T. Grosan, I. Pop, Free convection in shallow and slender porous cavities filled by a nanofluid using Buongiorno's model, ASME J Heat Transf. 136 (2014) 082501.

[35] M.A. Sheremet, H.F. Oztop, I. Pop, MHD natural convection in an inclined wavy cavity with corner heater filled with a nanofluid, J. Magn. Magn. Mater. 416 (2016) 37–47.

[36] M. Ghalambaz, H. Hendizadeh, H. Zargartalebi, I. Pop, Free convection in a square cavity filled with a tridisperse porous medium, Transp. Porous Med. 116 (2016) 1–14.

[37] M. Ghalambaz, M. Sabour, I. Pop, Free convection in a square cavity filled by a porous medium saturated by a nanofluid: viscous dissipation and radiation effects, Eng. Sci. Technol., Int. J. 19 (2016) 1243–1253.

[38] A. Kasaeian, R. Danesh Azarian, O. Mahian, L. Kolsi, A.J. Chamkha, S. Wongwises, I. Pop, Nanofluid flow and heat transfer in porous media: A review of the latest developments, Int. J. Heat Mass Transf. 107 (2017) 778–791.

[39] A.I. Alsabery, P.G. Siddheshwar, H. Saleh, I. Hashim, Transient free convective heat transfer in nanoliquid-saturated porous square cavity with a concentric solid insert and sinusoidal boundary condition, Superlattices Microstruct. 100 (2016) 1006–1028.

[40] T. Basak, S. Roy, T. Paul, I. Pop, Natural convection in a square cavity filled with a porous medium: Effects of various thermal boundary conditions, Int J Heat Mass Transf. 49 (2006) 1430–1441.

[41] T. Javed, M. Arshad Siddiqui, Z. Mehmood, I. Pop, MHD natural convective flow in an isosceles triangular cavity filled with porous medium due to uniform/non-uniform heated side walls, J. Phys. Sci. 70 (2016) 919–928, http://dx.doi.org/10.1515/zna-2015-0232.

[42] A.I. Alsabery, A.J. Chamkha, H. Saleh, I. Hashim, B. Chanane, Effects of finite wall thickness and sinusoidal heating on convection in nanofluid-saturated local thermal non-equilibrium porous cavity, Physica A 470 (2017) (2017) 20–38.

[43] X. Zhang, W. Liu, New criterion for local thermal equilibrium in porous media, J. Thermophys. Heat Transf. 22 (2008) 649–653.

[44] A.I. Alsabery, H. Saleh, I. Hashim, P.G. Siddheshwar, Transient natural convection heat transfer in nanoliquid-saturated porous oblique cavity using thermal non-equilibrium model, Int. J. Mech. Sci. 112 (2016) 223–245.

[45] M. Sheremet, I. Pop, Conjugate natural convection in a square porous cavity filled by a nanofluid using Buongiorno's mathematical model, Int. J. Heat Mass Transf. 79 (2014) 137–145.

[46] I.A. Aleshkova, M.A. Sheremet, Unsteady conjugate natural convection in a square enclosure filled with a porous medium, Int J Heat Mass Transf. 53 (2010) 5308–5320.

[47] A.M.J. Al-Zamily, Analysis of natural convection and entropy generation in a cavity filled with multi-layers of porous medium and nanofluid with a heat generation, Int. J. Heat Mass Transf. 106 (2017) 1218–1231.

[48] A.J. Chamkha, A. Doostanidezfuli, E. Izadpanahi, M. Ghalambaz, Phase-change heat transfer of single/hybrid nanoparticles-enhanced phase-change materials over a heated horizontal cylinder confined in a square cavity, Adv. Powder Technol. 28 (2017) 385–397.

[49] K. Kalidasan, P. Rajesh, Kanna, Natural convection on an open square cavity containing diagonally placed heaters and adiabatic square block and filled with hybrid nanofluid of nanodiamond-cobalt oxide/water, Int. Commun. Heat Mass Transf. 81 (2017) 64–71.

[50] M.R. Rahman, L. Abdul, I. Kin Yuen, S. Azam Che, R. Mohd, Thermal fluid dynamics of Al_2O_3–Cu/Water hybrid nanofluid in inclined lid driven cavity, J. Nanofluids 6 (2017) 149–154.

[51] D.A. Nield, A.V. Kuznetsov, The Cheng-Minkowycz problem for natural convective boundary-layer flow in a porous medium saturated by a nanofluid, Int. J. Heat Mass Transf. 52 (2009) 5792–5795.

[52] A.V. Kuznetsov, D.A. Nield, The Cheng-Minkowycz problem for natural convective boundary layer flow in a porous medium saturated by a nanofluid: a revised model, Int. J. Heat Mass Transf. 68 (2013) 682–685.

[53] D.A. Nield, A.V. Kuznetsov, Thermal instability in a porous medium layer saturated by a nanofluid: a revised model, Int. J. Heat Mass Transf. 68 (2014) 211–214.

[54] M.A. Sheremet, S. Dinarvand, I. Pop, Effect of thermal stratification on free convection in a square porous cavity filled with a nanofluid using Tiwari and Das' nanofluid model, Physica E: Low-Dimensional Syst. Nanostruct. 69 (2015) 332–341.

[55] D.A. Nield, A. Bejan, Convection in Porous Media, Springer, New York, 2013.

[56] J.N. Reddy, An introduction to the finite element method, McGraw-Hill, New York, 1993.

[57] S. Rao, The finite element method in engineering, Butterworth-Heinemann, 2005.

[58] P. Wriggers, Nonlinear finite element methods, Springer Science and Business Media, 2008.

[59] J. Donea, A. Huerta, Finite element method for flow problems, J, Wiley, 2003.

[60] O. Turan, A. Sachdeva, N. Chakraborty, R.J. Poole, Laminar natural convection of power-law fluids in a square enclosure with differentially heated side walls subjected to constant temperatures, J. Nonnewton. Fluid Mech. 166 (2011) 1049–1063.